Spectroscopic Study of Ni-rich Al-Co-Ni Quasicrystal

K. SODA*†, M. INUKAI‡⊥, M. KATO†, S. YAGI†, Y.-G. SO§+ and K. EDAGAWA§

†Department of Quantum Engineering, Graduate School of Engineering, Nagoya University, Furo-cho, Chikusa-ku, Nagoya 464-8603, Japan
‡Venture Business Laboratory, Nagoya University, Furo-cho, Chikusa-ku, Nagoya 464-8603, Japan
§Institute of Industrial Science, The University of Tokyo, 4-6-1 Komaba, Meguro-ku, Tokyo 153-8505, Japan

*Corresponding author. E-mail: j45880a@nucc.cc.nagoya-u.ac.jp
Telephone: +81-52-789-4683, Fax: +81-52-789-5155

⊥Present address: Japan Synchrotron Radiation Research Institute, 1-1-1 Kouto, Sayo-cho, Sayo-gun, Hyogo 679-5198, Japan; inukai.manabu.47@spring8.or.jp

+Present address: National Institute for Materials Science, 1-1 Namiki, Tsukuba 305-0044, Japan; SO.Yeonggi@nims.go.jp

(Received 30 May 2010; final version received 2010)

Valence-band electronic structure of a decagonal Ni-rich Al-Co-Ni quasicrystal, $Al_{72}Co_8Ni_{20}$, has been investigated by soft x-ray photoelectron spectroscopy. In particular the energy distributions of the transition-metal 3*d* bands have been focussed on by the Co and Ni 2*p*-3*d* resonance photoemission and they have been compared with those calculated by the discrete variational $X\alpha$ method for a model cluster based on a proposed Ni-rich Al-Co-Ni approximant, as well as the 3*d* band observed in the Co-rich Al-Co-Ni qusicrystal $Al_{72}Co_{16}Ni_{12}$. In the Ni-rich Al-Co-Ni, the transition-metal 3*d* band is peaked at the binding energy E_B of 2.3 eV, which is higher than that of the Co-rich Al-Co-Ni. The observed Ni 3*d* band has a single-peaked distribution around E_B ~ 2.4 eV in contrast to the calculated bimodal and wide-spread distribution for the proposed Ni-rich Al-Co-Ni model cluster, while the Co 3*d* band is located at E_B ~ 1.7 eV, consistent with the model calculation.

Keywords: valence-band electronic structure; soft x-ray photoelectron spectroscopy; DV-$X\alpha$ cluster calculation; decagonal quasicrystal; $Al_{72}Co_8Ni_{20}$

1. Introduction

A decagonal Al-Co-Ni alloy is one of the most intensively studied two-dimensional quasicrystals (QC) [1], where their quasiperiodic planes are stacked periodically along a tenfold axis (*c*-axis); the atomic arrangement in the plane may be constructed by a special tiling such as the well-known Penrose one with two unit tiles of fat and skinny rhombi or viewed as consisting of one unit cluster with an overlap rule [2]. Various

structural modifications have been also observed as a function of the Co/Ni ratio by high-resolution transmission electron microscopic (HRTEM) studies [1,3]. Decagonal (pentagonal) Al-transition metal (TM) mixed ring-like arrangement is found for the unit cluster center of the Co-rich Al-Co-Ni QC [1,4,5], while the symmetry breaking of the decagonal cluster center is recognized for the Ni-rich one [6]. The origin of these modifications have been studied by a Monte Carlo calculation with the interatomic pair potentials [7-9], which shows a preferential decagonal Al-TM arrangements in the Co-rich Al-Co-Ni QC and the hexagon-boat-star (HBS) tiling with a Ni-Ni pair arrangement in the Ni-rich one. The importance of the energetically favourable Al-Co and Ni-Ni interactions as well as the contribution of the Hume-Rothery mechanism to the structural stabilization are also pointed out by electronic band structure calculations for Al-Co-Ni approximants [10] and a recent *ab intio* study of a W-(AlCoNi) approximant $Al_{72.5}Co_{20}Ni_{7.5}$ [11]. The broken symmetry in the Ni-rich Al-Co-Ni QC may be caused by the chemical ordering between Al and TM [12,13]. However, it is still challenging to clarify the unique atomic arrangement and its formation mechanism, because of the lack of periodicity and of the difficulty in distinguishing between the constituent TM's by electron microscopy.

Thus we have studied the electronic structure and TM arrangement of the decagonal QC by comparing spectroscopic data with the electronic structure calculated for model unit clusters based on microscopic observation. The TM arrangement was studied first by Krajči *et al*. [10] by comparison of the electronic structure calculated for a large $Al_{70}Co_{15}Ni_{15}$ approximant with ultraviolet photoelectron spectroscopic (UPS) data, which was available at that time. However, the detailed structural modification with the Co/Ni ratio was not explicitly taken into account and it was found later that the TM 3*d* band in UPS is different from that in x-

ray photoelectron spectroscopy (XPS) [14] because of the difference in the surface sensitivity between UPS and XPS. Although the electronic structure of the Al-Ni-Co QC was also studied by soft x-ray emission and absorption spectroscopy (XES and XAS) [15] and electron energy loss spectroscopy (EELS) [16], the Co/Ni-ratio dependence of the electronic structure is out of their scope. In our previous studies on the Co-rich Al-Co-Ni QC [14,17-19], we found that the Al coordination around TM lowers the energy of the TM 3*d* states and that the very small difference in the bond energy between the occupations of Ni and Co at the TM sites in the central decagonal ring suggests that the chemical disordering may easily occur between Ni and Co.

In this paper, we will show results obtained by XPS, in particular the TM 2*p*-3*d* resonance photoemission, and by cluster calculation for the Ni-rich QC. We will also compare them with the XPS and XES results for the Co-rich QC. In general, a total density of states (DOS) may be given by a normal XPS spectrum, where the TM 3*d* band is prominent because of its high DOS and large photoionization cross section, while the TM 2*p*-3*d* resonance XPS may decompose the TM 3*d* band into the constituent 3*d* partial DOS's [20], as described in detail later. The TM 3*d* partial DOS can be also estimated by TM 3*d*-2$p_{3/2}$ XES ($L\alpha$ XES) through the dipole selection rule for the optical transitions related to the TM 2*p* core levels [15], as shown in the previous reports [14,19].

2. Experimental and calculating procedures

The XPS measurement was performed at the beamline BL27SU of SPring-8 of Japan Synchrotron Radiation Research Institute [21]. Photoelectron spectra were recorded at 10 K in the angle-integrated mode with a hemispherical analyzer (PHOIBOS 150) and linearly polarized excitation photons from an undulator. Total energy resolution and

the origin of the binding energy, E_B, the Fermi energy E_F, were determined by measuring of the Fermi edge of evaporated Au films. The energy resolution was estimated to be 0.16 eV at the excitation photon energy $h\nu$ of ~1000 eV. The $Al_{72}Co_8Ni_{20}$ specimens of 1 x 1 x 3 mm^3 in size were cut from an ingot prepared by Ar arc-melting of appropriate mixture of constituent elements, annealing at 1170 K for 192 ks and water-quenching. We confirmed the specimens in basic Ni phase [1,3] by x-ray diffraction patterns. Their clean surfaces for the photoelectron measurement were obtained by *in situ* fracturing the specimens with a knife edge. This *in situ* fracturing procedure is commonly used for obtaining clean surfaces of solid materials in investigation of the bulk electronic structure by photoelectron spectroscopy: We believe that it may provide us a proper information on the bulk electronic structure, since it is expected that a fractured surface is less damaged than, for example, surfaces prepared by *in situ* scraping with a diamond file [22,23] to suppress the effects of the surface deterioration and preserve the bulk atomic arrangement, even though it is less well-ordered than surfaces prepared with a more sophisticated sputter-anneal method.

The electronic structure was calculated by the discrete variational $X\alpha$ (DV-$X\alpha$) method [24] with a commercially available code SCAT modified [17]. The DV-$X\alpha$ method is one of the first principle molecular orbital calculations, where the Hartree-Fock-Slater molecular equation is solved by the self-consistent charge procedure with the Slater's $X\alpha$ potential as the electron exchange-correlation and the random-sampling integration for the matrix elements of Hamiltonian and overlap integrals [24]. This method is powerful for the study on the electronic structure and chemical bonding in the materials including many TM's without periodicity. For applying the DV- $X\alpha$ method to the large cluster containing many TM's, such as the

present Al-Co-Ni quasicrystal, we have modified the available code SCAT for faster calculation with larger cluster than the original one [17].

The Al-Co-Ni cluster used for the calculation has a triple-layered structure, which is made up of two types of layers A and B, as shown in figure 1, in the stacking sequence of A-B-A or B-A-B layers. Figure 1 shows a unit bilayer (A-B layered) model cluster $Al_{72}Co_{11}Ni_{24}$ for the Ni-rich Al-Co-Ni QC: The atomic arrangement in each layer is based on a theoretical study by use of interatomic pair potentials for a Ni-rich approximant $Al_{70}Co_9Ni_{21}$ [9]. In figure 1, underlying Penrose and HBS tilings are also shown by broken and gray solid lines, respectively. In our calculation, the interlayer distance $c/2$ and the quasilattice constant a_q, the edge length of the rhombi, are set to 0.200 and 0.250 nm, respectively [1].

The electronic structure of the Ni-rich QC $Al_{72}Co_8Ni_{20}$ is obtained as the sum of the local DOS for the central A and B layers calculated for the respective B-A-B and A-B-A clusters to avoid the so-called surface effects. This procedure gives fairly good agreement with the band structure calculation [10,18], in particular, for the relation between the spectral feature of the TM 3*d* DOS and the TM arrangement. Furthermore, we extracted the local TM 3*d* DOS's for eleven Co and four Ni in the inner part of the layer and obtained the partial TM 3*d* DOS for the Ni-rich model cluster, $Al_{72}Co_8Ni_{20}$, by multiplying their concentration factors. This is because the TM 3*d* DOS is sensitive to the Al coordination and hence the TM atoms in the peripheral part of the cluster layer may show their incorrect energy distribution (one of the surface effects) [18,19]. Finally, the calculated line spectra are convoluted with a Gaussian function of the 0.17 eV half width at half maximum to present the DOS's for comparison with the previous reports [14, 17-19] on the Co-rich Al-Co-Ni.

3. Results and discussion

Figure 2 shows typical XPS spectra for an off-resonance spectrum (curves), whose excitation photon energy $h\nu$ is 1000.87 eV, and anti-resonance spectra (dots) recorded on the photoexcitation slightly below the Co and Ni 2*p* thresholds, $h\nu$ = 776.94 and 851.57 eV, respectively. These spectral intensity are normalized around E_B = 11 eV, where the primary XPS signals are not observed. In the anti-resonance spectra, one notice that the main TM 3*d* band at E_B ~ 2.3 eV is reduced and changed in the spectral shape and that the satellite structures appears in the high binding energy side of the main band. These are attributed to the well-known 2*p*-3*d* resonance photoemission [20]; it may occur through the quantum interference effect between the direct excitation (normal photoemission) of the 3*d* electron to the continuum and its indirect excitation via an Auger-like direct recombination transition of the intermediate excited states $\underline{2p}3d^{n+1}$. Here, $\underline{2p}$ denotes a hole in the 2*p* core level, which would be made virtually by photoabsorption, and *n* the number of the *d* electrons in the initial states. Thus the TM 3*d* photoemission intensity may be reduced in the pre-threshold region (referred to as the anti-resonance) and resonantly enhanced at the 2*p* threshold (the on-resonance). In turn the partial TM 3*d* DOS may be obtained from comparison of the on- or anti-resonance spectra with the off-resonance one recorded at the excitation photon energy sufficiently far from the threshold. In the present study, we have subtracted the anti-resonance spectra from the off-resonance one, because (1) the huge resonant Auger signals overlap with the main TM 3*d* band at the on-resonance region and (2) the resonance enhancement of the Ni 3*d* main band is small due to the high initial $3d^{10}$ configuration [14, 20, 25]. Thus obtained results are also shown as difference spectra in figure 2. In the Ni-rich Al-Co-Ni QC, the TM 3*d* band is extended from E_F to ~5 eV with a single peak at E_B ~ 2.3 eV and composed of the Ni

and Co 3*d* bands peaked at E_B ~ 2.4 eV and 1.7 eV, respectively, as shown by vertical broken lines. Although the present normalization procedure neglects an apparent intensity change in the higher binding energy region due to the secondary electrons, it does not affect their overall spectral features so much.

In figure 3, experimentally obtained total and partial DOS's of the TM 3*d* states of the Ni-rich Al-Co-Ni QC are compared with those calculated for the Ni-rich model cluster as well as the previously reported results for a Co-rich QC $Al_{72}Co_{16}Ni_{12}$ [14]. Here, the experimental total DOS's (thick curves) are presented, after smoothing raw data shown in figure 2, by the off-resonance photoelectron spectra, and the Ni and Co 3*d* partial DOS's (curves with and without open circles, respectively) are estimated from the TM 2*p*-3*d* resonance XPS for the Ni-rich QC and from the TM $L\alpha$ XES for the Co-rich QC [14] and plotted so that the ratio of their integrated intensities may coincide with their concentration ratio. In the Ni-rich QC, the total TM 3*d* band is located at E_B ~ 2.3 eV, while that in the Co-rich QC is peaked around 1.9 eV. However, the partial distributions of the Co and Ni bands in the Ni-rich QC are similar to those in the Co-rich one.

On the other hand, as seen in the lowest panel of figure 3, the present calculation for the Ni-rich cluster predicts the bimodal and wide-spread Ni 3*d* partial DOS and the single-peaked Co one; a pseudogap near E_F for the Al partial DOS is also found consistently with the so far reported band structure calculation [10], suggesting the Hume-Rothery mechanism for the stabilization of the Ni-rich QC. The calculated spectral distribution of the Co 3*d* states agrees well with the experimental one but that of the Ni 3*d* states does not so well. The calculated bimodal distribution comes from the Ni-Ni bonding and anti-bonding states, as shown in figure 4, which shows the overlap populations between Ni and its neighbouring Ni and Al. Following

the Mulliken population analysis [26], the overlap population of a molecular orbital l in an LCAO (linear combination of atomic orbitals) scheme is defined as $C^*_{\mu l} C_{\nu l} S_{\mu\nu}$, where $C_{\mu l}$, $C_{\nu l}$, and $S_{\mu\nu}$ stand for the expansion coefficients of the basis atomic orbitals μ and ν, and their overlap integral, respectively. In the present study, the positive (bonding) and negative (anti-bonding) overlap populations are separately summed up for the appropriate bases μ and ν of the relevant atoms within the interatomic distance of 0.4 nm, beyond which the overlap integrals are negligibly small. The contribution of the anti-bonding states appearing at $E_B \sim 1$ eV may be overestimated in the present calculation, because the present Ni-rich model cluster contains only the Ni-Ni pairing configuration (a pair of open and closed diamonds in figure 1). Furthermore, the Ni-Al overlap population in figure 4 also indicates lowering the Ni 3*d* band due to the Ni-Al interaction, and the previous study for the Co-rich QC [18] shows that the Ni 3*d* band of a single Ni configuration may appear $E_B = 2 \sim 3$ eV. Thus the observed spectral shape of the Ni 3*d* band of the Ni-rich QC may indicate the large contribution of the single Ni configuration together with that of the Ni-Ni pairing configuration, or the spectral difference in the TM 3*d* bands of the Ni- and Co-rich QC's might be explained by the simple difference in their Co and Ni concentrations without changing the spectral shapes of TM partial DOS, *i.e*. by single TM configurations. The TM $L\alpha$ XES measurement, which is more bulk-sensitive than XPS, will provide us further information on the TM 3*d* partial DOS.

4. Summary

We have investigated the energy distribution of Ni and Co 3*d* states by the 2*p*-3*d* resonance XPS measurement and DV-$X\alpha$ cluster calculation for the Ni-rich Al-Co-Ni QC. The DV- $X\alpha$ calculation for a Ni-rich model cluster shows the bimodal Ni 3*d*

partial DOS due to the Ni-Ni interaction, which is not clearly observed in the present XPS spectra, while the calculated Co 3*d* DOS agrees well with the experimental one.

Further study on the TM 3*d* partial DOS is intended by TM $L\alpha$ XES measurement.

Acknowledgements
The soft x-ray photoelectron measurements were performed at the beamline BL27SU of SPring-8 with the approval of the Japan Synchrotron Radiation Research Institute (JASRI) (Proposal Nos. 2009A1672 and 2009B1729).

Figure Captions

Figure 1. Unit bilayer cluster model of Ni-rich Al-Co-Ni quasicrystal, $Al_{72}Co_{11}Ni_{24}$. An underlying Penrose tiling of fat and skinny rhombi is presented by broken lines and an HBS (Hexagon-Boat-Star) tiling is also shown by gray lines. Open and closed symbols stand for atoms located in the lower A and higher B layers (z = 0 and c/2, where c is a lattice constant in the periodic direction), respectively. A large circle represents the cluster radius of ~2 nm.

Figure 2. Valence-band photoelectron spectra (dots) recorded at the Co and Ni 2*p*-3*d* anti-resonance photon energies $h\nu$ of 776.94 and 851.57 eV, respectively, and (curves) at an off-resonance photon energy of 1000.87 eV. Difference spectra are also shown by curves with and without open circles between the off- and anti-resonance spectra at the Ni and Co 2*p*-3*d* thresholds, respectively. Broken lines indicate the location of the band in the difference spectra.

Figure 3. Comparison of experimental and theoretical total and partial densities of states (DOS's) of Ni-rich Al-Co-Ni quasicrystal (QC) $Al_{72}Co_{8}Ni_{20}$ (the lowest and middle panels). Experimental DOS's for Co-rich QC $Al_{72}Co_{16}Ni_{12}$ (taken form [14]) were also shown in the uppermost panel. Photoelectron spectra are presented as the total DOS's by thick curves, and the Co 3*d* (curves) and Ni 3*d* (curves with circles) partial DOS's are estimated from their 2*p*-3*d* resonance photoemission for Ni-rich QC and from their $L\alpha$ x-ray emission for Co-rich QC [14]. The theoretical partial densities of Al, Co, and Ni states calculated for Ni-rich QC $Al_{72}Co_{8}Ni_{20}$ are presented by a dotted curve and curves without and with circles, respectively, and total one as their sum by a thick curve. Broken lines indicate the positions of the experimental Ni and Co 3*d* bands.

Figure 4. Overlap population between Ni and its neighbouring Ni and Al in Ni-rich Al-Co-Ni model cluster. Partial densities of states of Al and Ni are shown for comparison in the upper panel.

References

[1] K. Hiraga, Adv. Imaging and Electron Phys. **122** (2002) p.1.
[2] H.-C. Jeong and P.J. Steinhardt, Phys. Rev. B **55** (1997) p.3520.
[3] S. Ritsch, C. Beeli, H.-U. Nissen, T. Godecke, M. Scheffer and R. Luck, Phil. Mag. Lett **78** (1998) p.67.

[4] K. Sugiyama, S. Nishimura and K. Hiraga, J. Alloys Comp. **342** (2002) p.65.
[5] S. Deloudi, M. Kobas and W. Steuer, Phil. Mag. (2006) p.581.
[6] E. Abe, K. Saitoh, H. Takakura, A.P. Tsai, P.J. Steinhardt and H.-C. Jeong, Phys. Rev. Lett. **84** (2000) p.4609.
[7] S. Hiramatsu and Y. Ishii, J. Phys. Soc. Jpn. **75** (2006) p.054602.
[8] N. Gu, C.L. Henley and M. Mihalkovič, Phil. Mag. **86** (2006) p.593.
[9] M. Mihalkovič, I. Al-Lehyani, E. Cockaye, C.L. Henley, N. Morghadam, J.A. Moriarty, Y. Wang and M. Widom, Phys. Rev. B **65** (2002) p.104205.
[10] M. Krajči, J. Hafner and M. Mihalkovič, Phys. Rev. B **62** (2000) p.243.
[11] K.H. Hassdenteufel, A.R. Oganov, S. Katrych and W. Steurer, Phys. Rev. B 75 (2007) p.144115.
[12] E. Abe, K. Saitoh, H. Takakura, A.P. Tsai, P.J. Steinhardt and H.-C. Jeong, Phys. Rev. Lett. **84** (2000) p.4609.
[13] Y. Yan and S.J. Pennycook, Phys. Rev. Lett. **86** (2001) p.1542.
[14] M. Inukai, K. Soda, S. Ota, H. Miyazaki, T. Suzuki, M. Kato, S. Yagi, Y. Tezuka, Y. Yokoyama, Phil. Mag. **87** (2007) p.3003.
[15] E. Belin-Ferre, Z. Dankhazi, V. Fournee, A. Sadoc, C. Berger, H. Müller, H. Kirchmayr, J. Phys.: Condens. Matter **8** (1996) p.6213.
[16] M. Terauchi, Y. Uemichi, H. Ueda, A.P. Tsai, T. Takeuchi, U. Mizutani, Phil. Mag. **87** (2007) 2947.
[17] M. Inukai *et al*., Adv. Microsc. Theor. Calc. Lett. 1 (2008) p.156.
[18] M. Inukai, K. Soda, M. Kato, S. Yagi and Y. Yokoyama, Z. Krist. **223** (2008) p.851.
[19] M. Inukai, K. Soda, M. Kato, S. Yagi, Y. Tezuka, Y. Yokoyama, T. Muro and Y. Saitoh, J. Phys.: Conf. Ser. *in press*.
[20] S. Hüfner, *Photoelectron Spectroscopy: Principles and Applications*, 3rd ed. Springer Verlag, Berlin, 2003.
[21] H. Ohashi, E. Ishiguro, H. Okumura, A. Hiraya, Y. Senba, K. Okada, N. Saito, I. Suzuki, K. Ueda, T. Ibuki, S. Nagaoka, I. Koyano and T. Ishikawa, Nucl. Instrum. Methods A **467** (2001) p.533.
[22] K. Soda, H. Murayama,S. Yagi,M. Kato,T. Takeuchi,U. Mizutani,S. Imada, S. Suga,Y. Saitoh,T. Muro, H. Sumi, Y. Nishino, Physica B **351** (2004) p.338.
[23] H. Miyazaki, K. Soda, S. Yagi, M. Kato, T. Takeuchi, U. Mizutani, Y. Nishino, J. Vac. Sci. Technol. A **24** (2006) p.1464.
[24] H. Adachi, M. Tsukuda and C. Satoko, J. Phys. Soc. Jpn., **45** (1978) p.875.
[25] M. Magnuson, A. Nilsson, M. Weinelt and N. Martensson, Phys. Rev. B **60** (1999) p.2436.
[26] R. S. Mulliken, J. Chem. Phys. 23 (1955) p.1833, p.1841, p.2338 and p.2343.

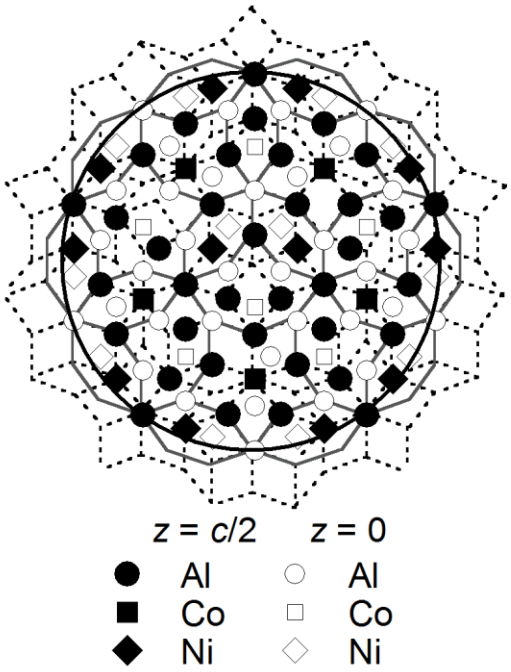
z = c/2
z = 0
Al
Co
Ni
Al
Co
Ni

Fig.1

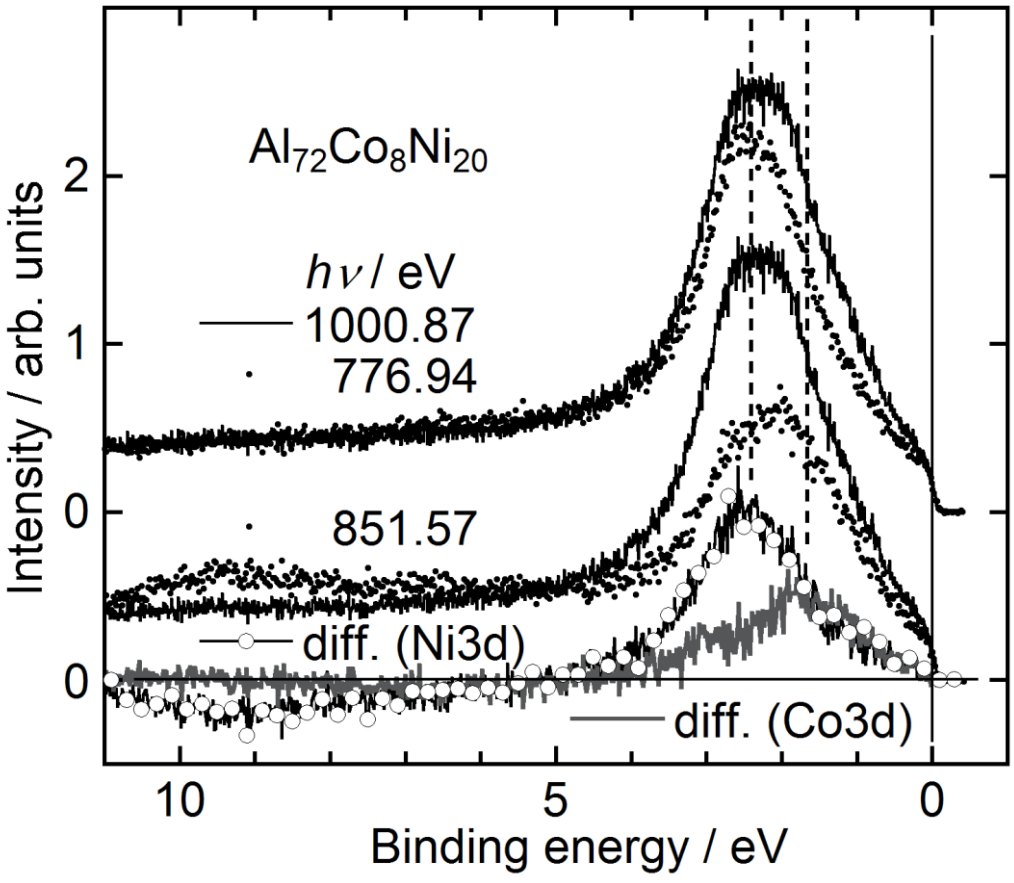
Al72Co8Ni20
hν / eV
1000.87
776.94
851.57
diff. (Ni3d)
diff. (Co3d)
Intensity / arb. units
Binding energy / eV
2
1
0
0
10
5
0

Fig.2

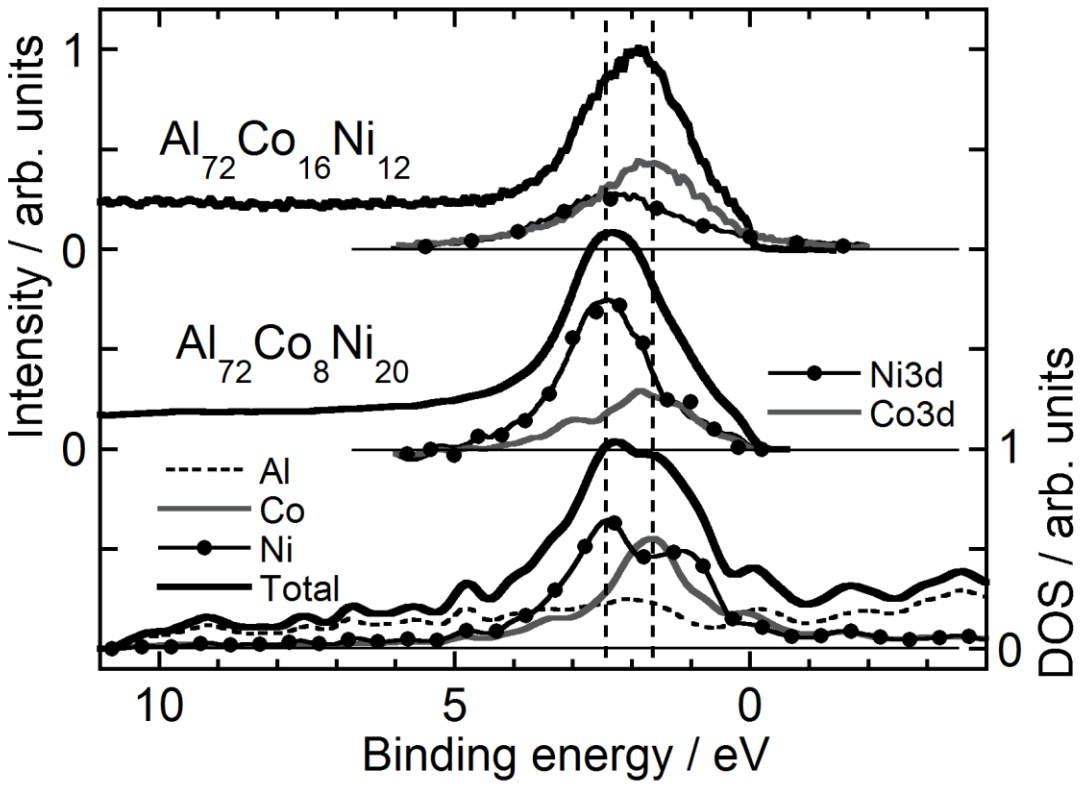
Intensity / arb. units
1
0
0
Al72Co16Ni12
Al72Co8Ni20
Ni3d
Co3d
Al
Co
Ni
Total
1
0
DOS / arb. units
10
5
0
Binding energy / eV

Fig.3

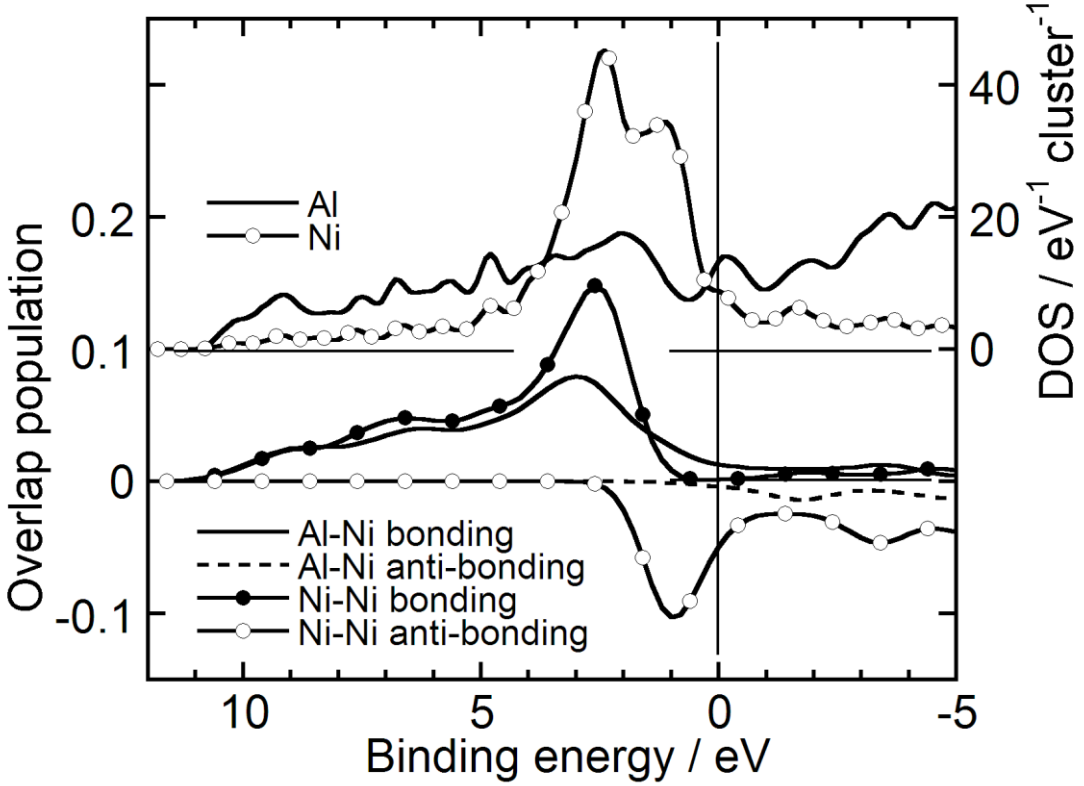
Overlap population
0.2
0.1
0
-0.1
Al
Ni
Al-Ni bonding
Al-Ni anti-bonding
Ni-Ni bonding
Ni-Ni anti-bonding
40
20
0
DOS / eV-1 cluster-1
10
5
0
-5
Binding energy / eV

Fig.4